Supplemental Figures

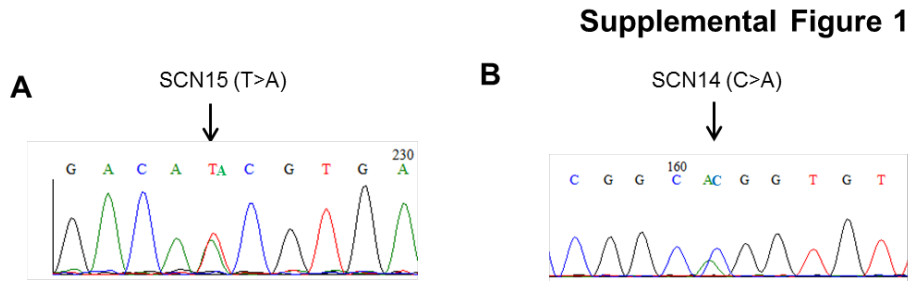

Supplemental Figure 1. Expressed *ELANE* mutations are retained in iPSC after the reprogramming process. (A-B) Chromatograms of *ELANE* exon 3 sequencing of genomic DNA derived from iPSC showing the T>A mutation (I118N) in the SCN15 (A) and the C>A mutation (Q98P) in the SCN14 (B) lines.

Supplemental Figure 2

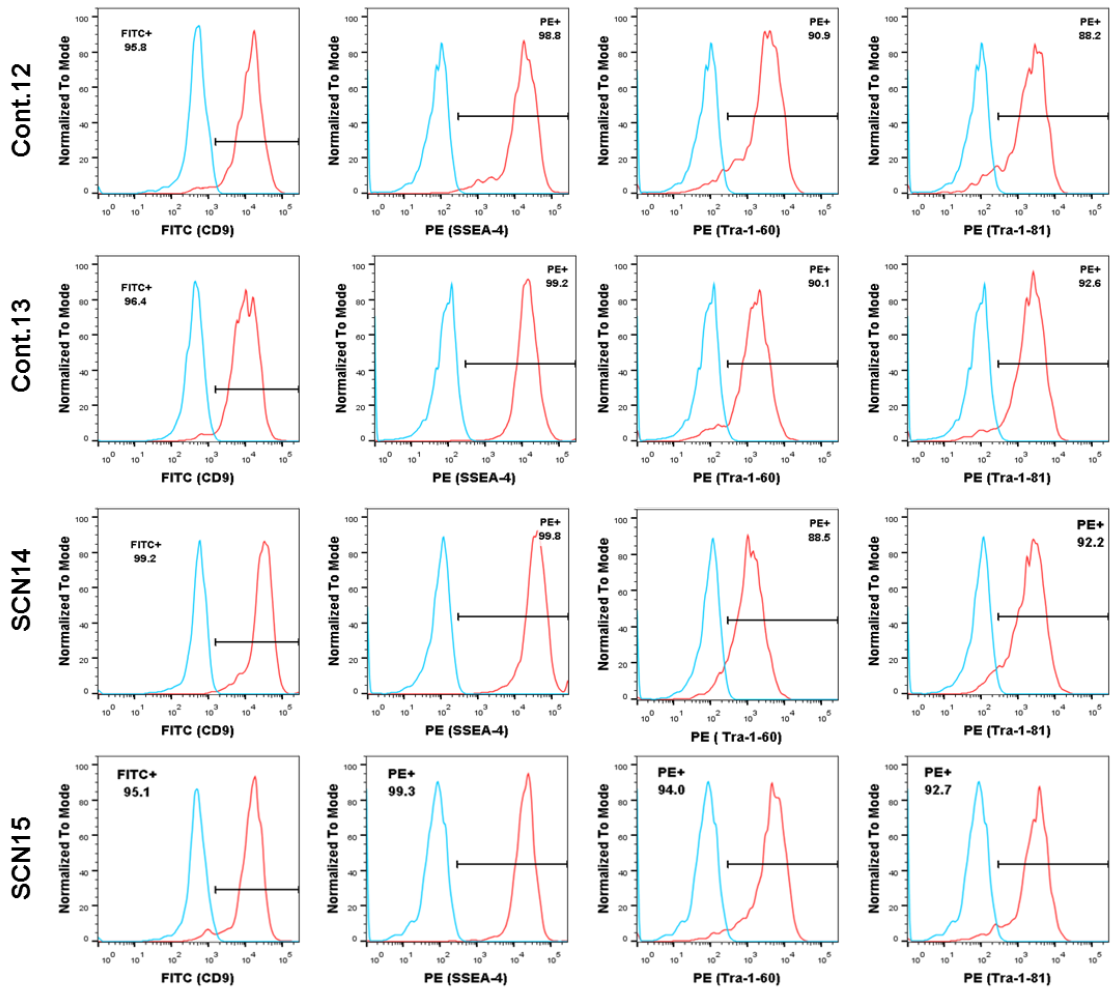

Supplemental Figure 2. iPSC lines show a phenotype compatible with pluripotency. Cont.12, Cont.13, SCN14 and SCN15 lines showed positive staining of the self-renewal markers CD9, SSEA-4, Tra-1-60, and Tra-1-81.

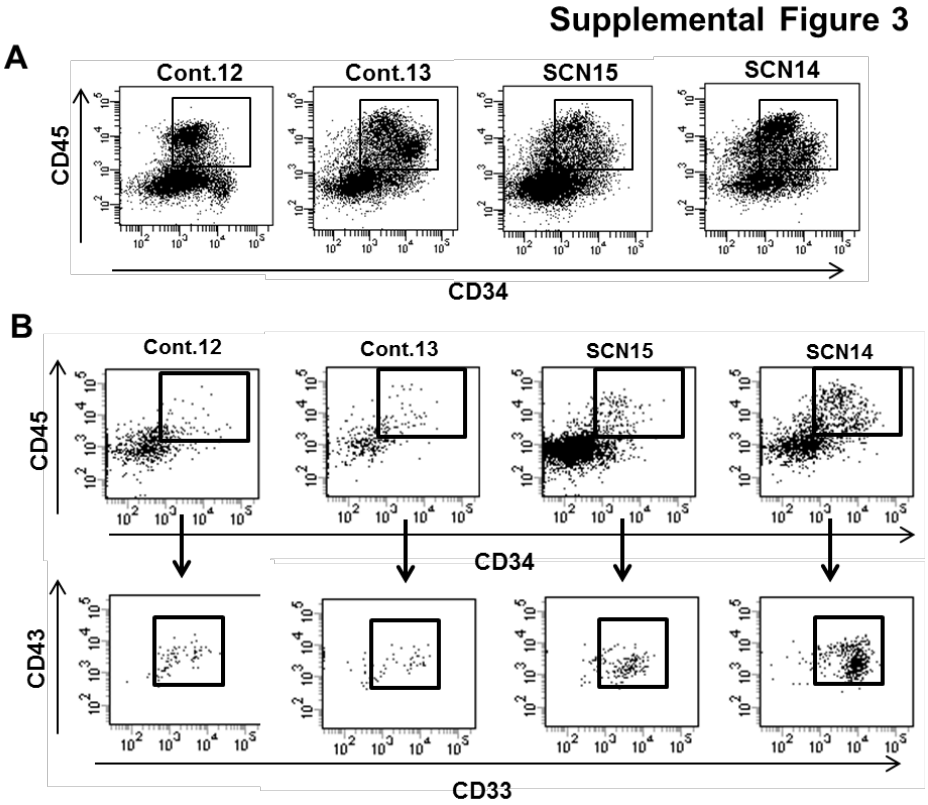

Supplemental Figure 3. Hematopoietic differentiation of healthy donor and *ELANE* Ex-3 mutant SCN patient derived iPSC. (A) The non-adherent cells at day 10 of the mesodermal and hematopoietic specific differentiation were FACS analyzed for hCD45 and hCD34 positive cells. (B) FACS dot plots showing the staining of hematopoietic progenitors for CD45, CD34, CD33, and CD43. The hematopoietic progenitors ($CD45^+/CD34^+$ cells) derived from the hematopoietic differentiation of iPSCs are positive for CD43 and CD33.

Supplemental Figure 4

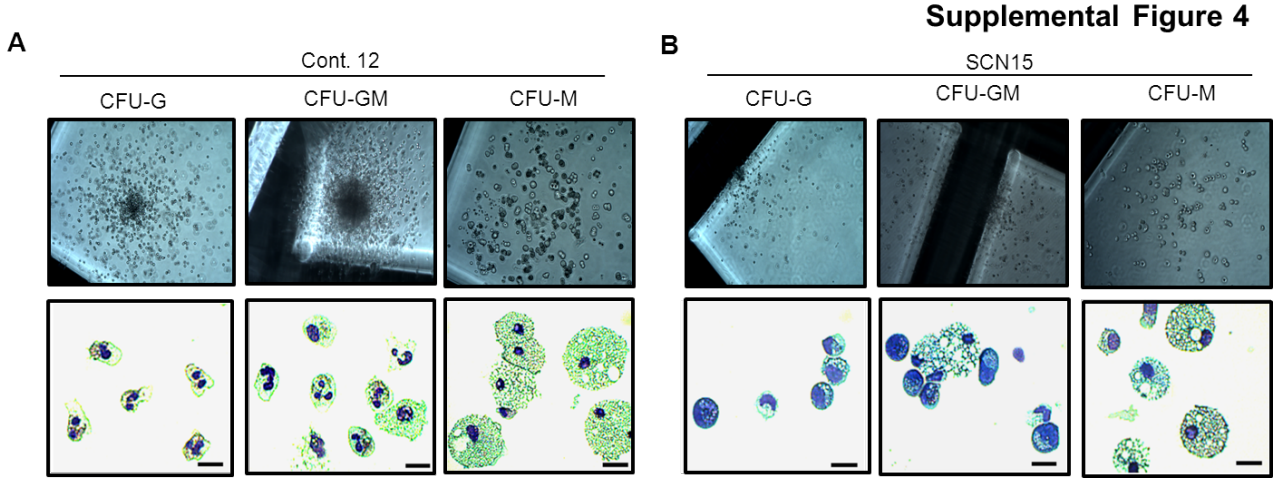

Supplemental Figure 4. Colony forming cells assay of the hematopoietic progenitors derived from healthy donor and *ELANE* exon-3 mutant SCN iPSCs. Cells were cultured in methyl cellulose semisolid medium containing cytokine mixture, and the myeloid (CFU-G, CFU-GM, CFU-M) and mix colonies were scored at day 14. (A) Control iPSC (Cont.12) derived CFU-G, CFU-GM and CFU-M containing mature neutrophils and macrophages. (B) *ELANE* I118N SCN iPSC (SCN15) derived CFU-G, CFU-GM and CFU-M containing macrophages and immature myeloid cells. Bars = 10 μm.

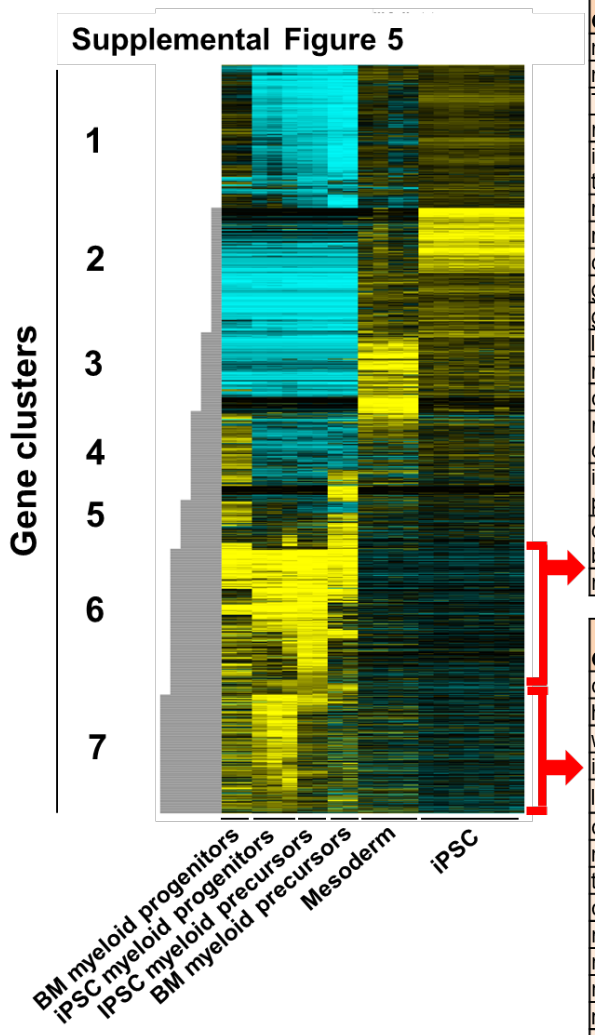

GO Biological processes	p(B-H FDR)	# genes in list
myeloid cell differentiation	2.15E-20	53
myeloid leukocyte activation	6.58E-18	34
T cell activation	1.08E-17	55
regulation of leukocyte activation	2.24E-17	53
immune response-activating signal transduction	4.06E-17	51
neutrophil chemotaxis	9.63E-17	23
neutrophil migration	1.99E-16	23
defense response to other organism	3.23E-16	51
granulocyte migration	7.18E-16	25
granulocyte chemotaxis	2.01E-14	23
leukocyte chemotaxis	2.09E-14	30
nucleosome assembly	3.05E-14	29
chromatin assembly or disassembly	6.43E-14	32
regulation of myeloid cell differentiation	6.43E-14	32
immune response-regulating signaling pathway	6.74E-14	53
defense response to Gram-positive bacterium	8.05E-14	21
regulation of leukocyte differentiation	8.36E-14	36

GO Biological processes	p(B-H FDR)	# genes in list
cell activation	1.61E-15	75
hemostasis	1.18E-10	47
wound healing	1.18E-10	54
innate immune response	1.18E-10	63
leukocyte migration	1.55E-10	35
cytokine-mediated signaling pathway	7.00E-08	35
myeloid leukocyte activation	2.71E-06	19
type I interferon signaling pathway	8.47E-06	13
cellular response to type I interferon	8.47E-06	13
response to type I interferon	9.38E-06	13
regulation of response to wounding	2.12E-05	29
regulation of cell migration	3.00E-05	36
negative regulation of catalytic activity	3.00E-05	45
regulation of intracellular signal transduction	3.10E-05	72
movement of cell or subcellular component	3.71E-05	78
regulation of cell motility	3.89E-05	37
hemopoiesis	4.21E-05	44

Supplemental Figure 5. Comparative transcriptome of BM promyelocytes and relevant hematopoietic populations derived from iPSC. A total of 1028 genes representing iPSC signature (black line cluster) are downregulated while 828 hematopoietic genes (red line cluster, GO analysis below) are upregulated in sorted myeloid progenitors (day 10) and promyelocytes (day 15) obtained from iPSC cultures compared with their counterparts in primary human BM (granulo-macrophagic progenitors and promyelocytes). Each lane represents an independent specimen and lanes are clustered according to their cell type.

Supplemental Figure 6

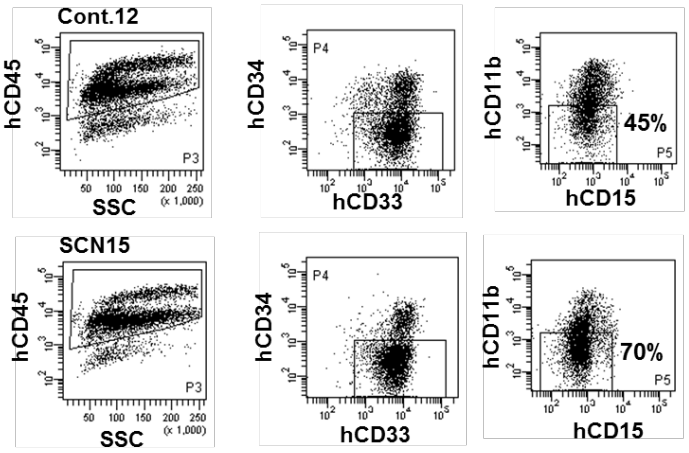

Supplemental Figure 6. Immunophenotypic analysis of granulopoietic differentiation. FACS dot plot of the granulopoietic differentiation of control/SCN iPSC derived hematopoietic progenitor cells. SCN iPSC derived cells show increased percentage of $CD45^{+}CD34^{-}CD33^{+}CD11b^{-}CD15^{lo}$ (promyelocytes/myelocytes) population as compared to control iPSC derived cells.

Supplemental Figure 7

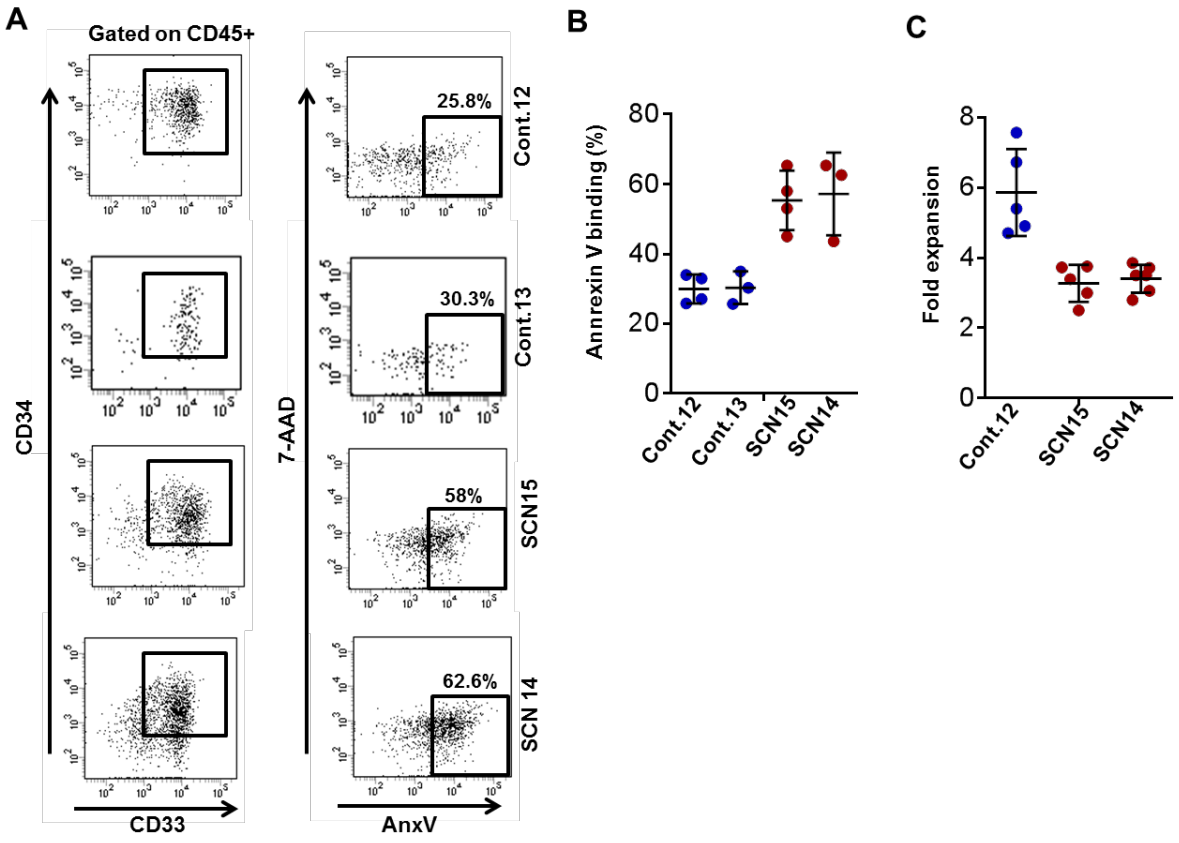

Supplemental Figure 7. Myeloid progenitors derived from hematopoietic differentiation of SCN iPSC have increased apoptosis in comparison to control iPSC derived myeloid progenitors. (A) FACS dot plots of annexin-V binding of myeloid progenitors derived from the control and *ELANE* exon-3 mutant SCN iPSCs. (B) Frequency of annexin-V^+ cells in control and SCN iPSC derived myeloid progenitors. (C) Analyses of the expansion of hematopoietic progenitors derived from control or SCN iPSCs in myeloid culture condition containing SCF, IL-3, and GM-CSF.

Supplemental Figure 8

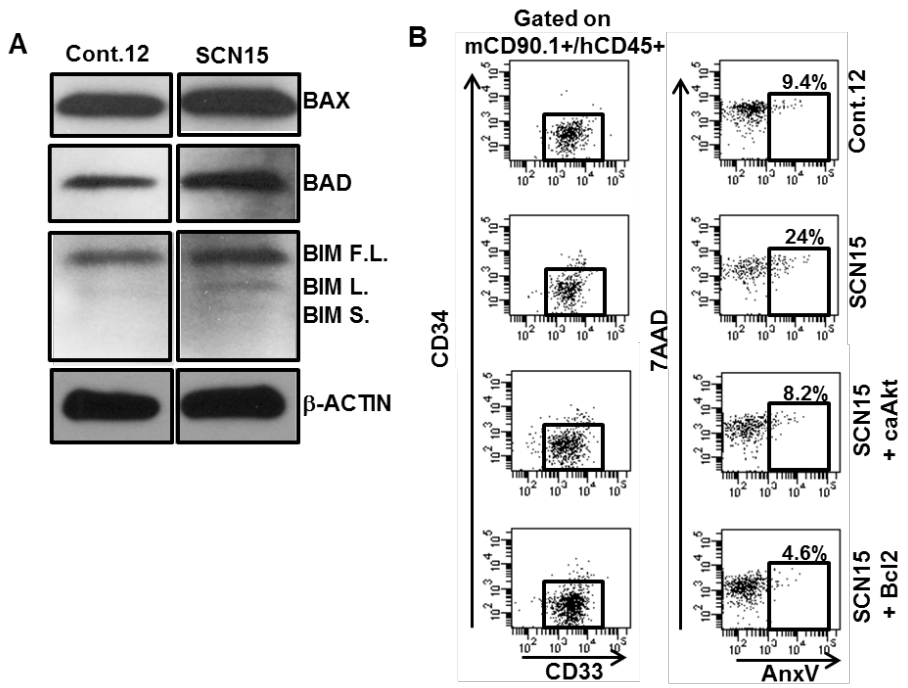

Supplemental Figure 8. Analyses of pro apoptotic protein expression and role Bcl2 and Akt in the survival of SCN iPSC derived promyelocytes. (A) Western blot of pro-apoptotic proteins BAX, BAD, and BIM in total cell lysates of promyelocytes derived from control (Cont.12) or *ELANE* I118N SCN iPSC (SCN15). (B) FACS dot plots of annexin-V binding of promyelocytes retrovirally transduced with constitutively active Akt (ca-Akt) or Bcl2. Hematopoietic progenitors derived from control and SCN iPSC at day 10 of differentiation were transduced with control vector or ca-Akt or Bcl2 retroviruses and cultured in the myeloid differentiation medium for 5 days, and analyzed for annexin-V binding of granulocytic precursors in all the groups.

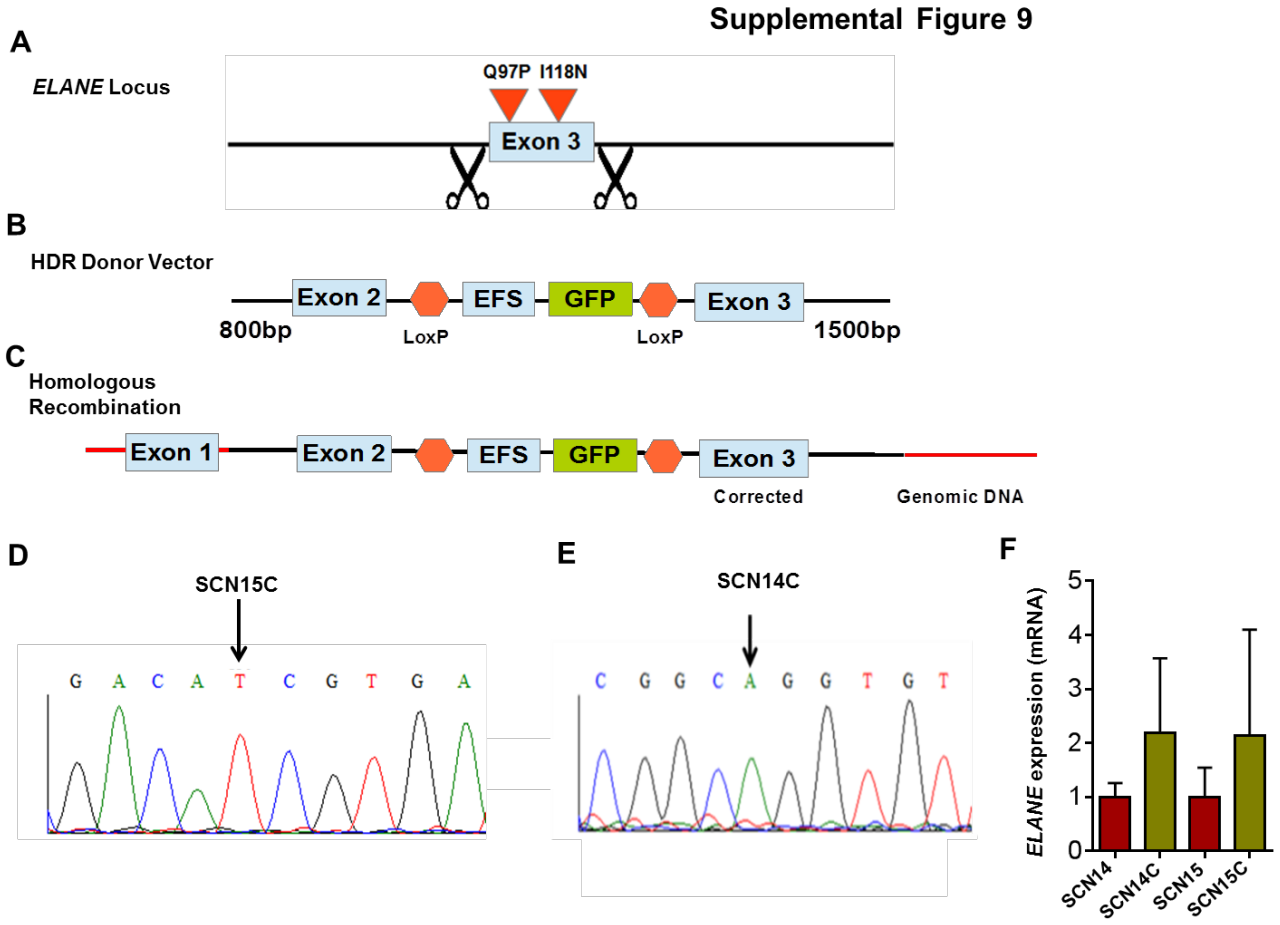

Supplemental Figure 9. CRISPR Design Schematic. (A) CRISPRS were designed to target either side of *ELANE* exon 3. (B) Donor vector design with wildtype *ELANE* sequence and a floxed EFS-GFP cassette to facilitate screening of donor insertion. (C) Representation of the final CRISPR corrected DNA. (D) Chromatograms of *ELANE* exon 3 sequencing of the cDNA generated from promyelocytes/myelocytes total RNA derived from SCN15 mutation corrected (SCN15C) line promyelocytes. (E) Chromatograms of *ELANE* exon 3 sequencing of the cDNA generated from promyelocytes/myelocytes total RNA derived from SCN14 mutation corrected (SCN14C) line promyelocytes. (F) Relative mRNA expression of NE in the promyelocytes/myelocytes derived from SCN iPSCs and SCN mutation corrected iPSCs. The quantitative real time PCR data of 3 independent experiments with duplicates are presented as mean ± SD.

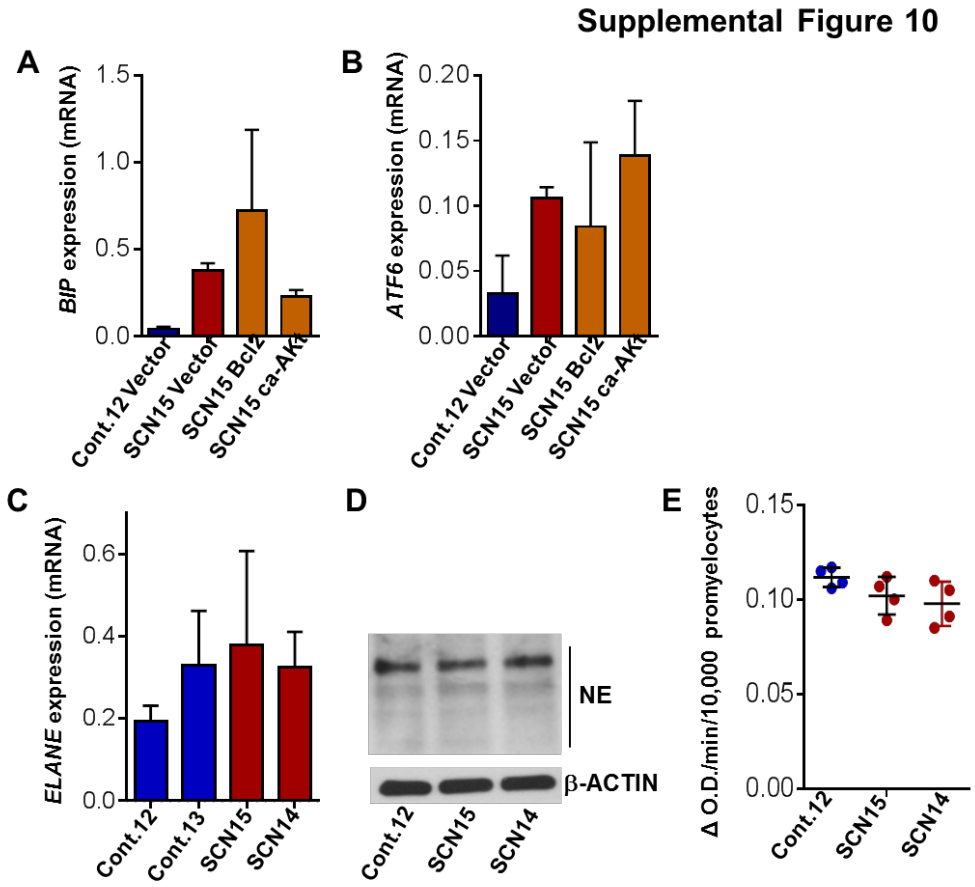

Supplemental Figure 10. ER stress is not restored by forced expression of Bcl2 or ca-Akt and the NE expression and activity of control and *ELANE* ex-3 mutant SCN iPSC derived granulocytic precursors are similar. (A-B) Expression of ER stress reporters *BIP* (A) and *ATF6* (B) in granulocytic precursors derived from Control 12 or SCN15 iPSC, transduced with an empty vector, Bcl2 or ca-Akt. The quantitative real time PCR data of two replicates from each of two independent experiments is presented. (C) Relative mRNA expression of NE in control and SCN iPSC derived promyelocytes/myelocytes. (D) Western blot analyses of neutrophil elastase (NE) in the lysate of promyelocytes derived from control or SCN iPSCs. Four bands are noticed between 29 and 50 KDa are noticed. This is the representative of two independently carried out western blots. (E) NE activity in the promyelocytes/myelocytes derived from control or SCN iPSC. The quantitative real time PCR data of 3 independent experiments in duplicate are presented as mean ± SD.

Supplemental Figure 11

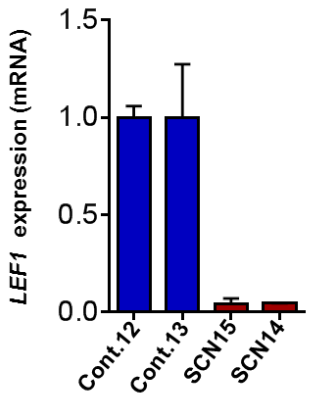

Supplemental Figure 11. SCN iPSC derived promyelocytes/myelocytes express reduced level of LEF1. Relative mRNA expression in the promyelocytes/myelocytes derived from control and SCN iPSC lines. The quantitative real time PCR data of 2 independent experiments in duplicate are presented as mean ± SD.

Supplemental Figure 12

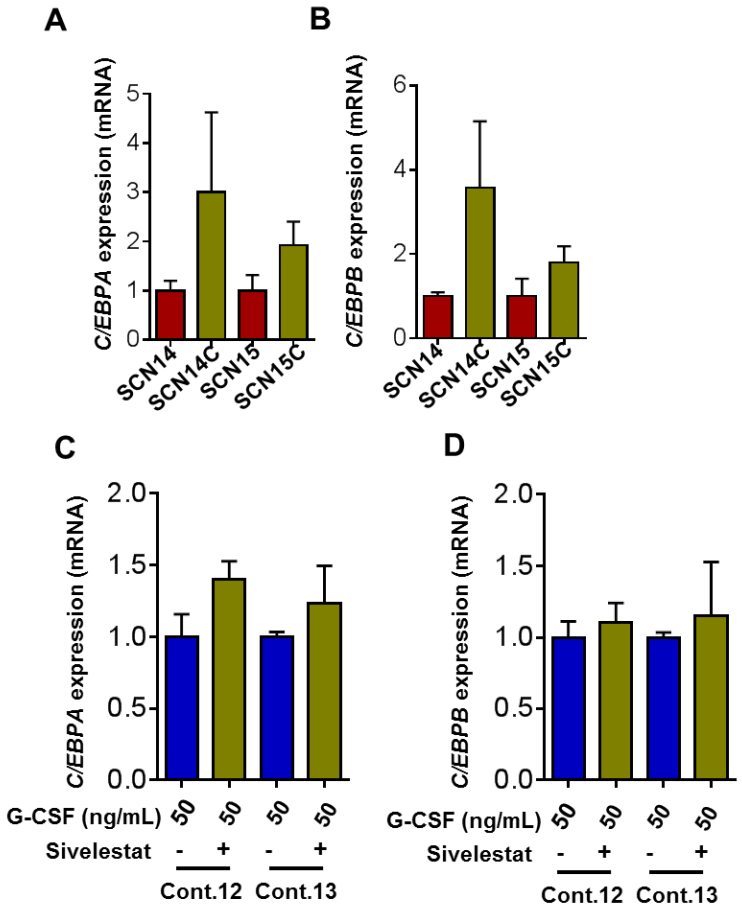

Supplemental Figure 12. Genetic correction of the mutations in exon-3 locus rescues the granulopoiesis by inducing the expression of *CEBPA* and *CEBPB*. (A) Relative expression of *CEBPA* mRNA in SCN15, SCN15C, SCN14 and SCN14C iPSC derived promyelocytes/myelocytes. (B) Relative expression of *CEBPB* mRNA in SCN15, SCN15C, SCN14, SCN14C iPSC derived promyelocytes/myelocytes. (C) Relative expression of *CEBPA* in control iPSC derived promyelocytes/myelocytes cultured in presence or absence of Sivelestat. Data are presented as mean ± SD of 2 or more independent experiments in duplicate.

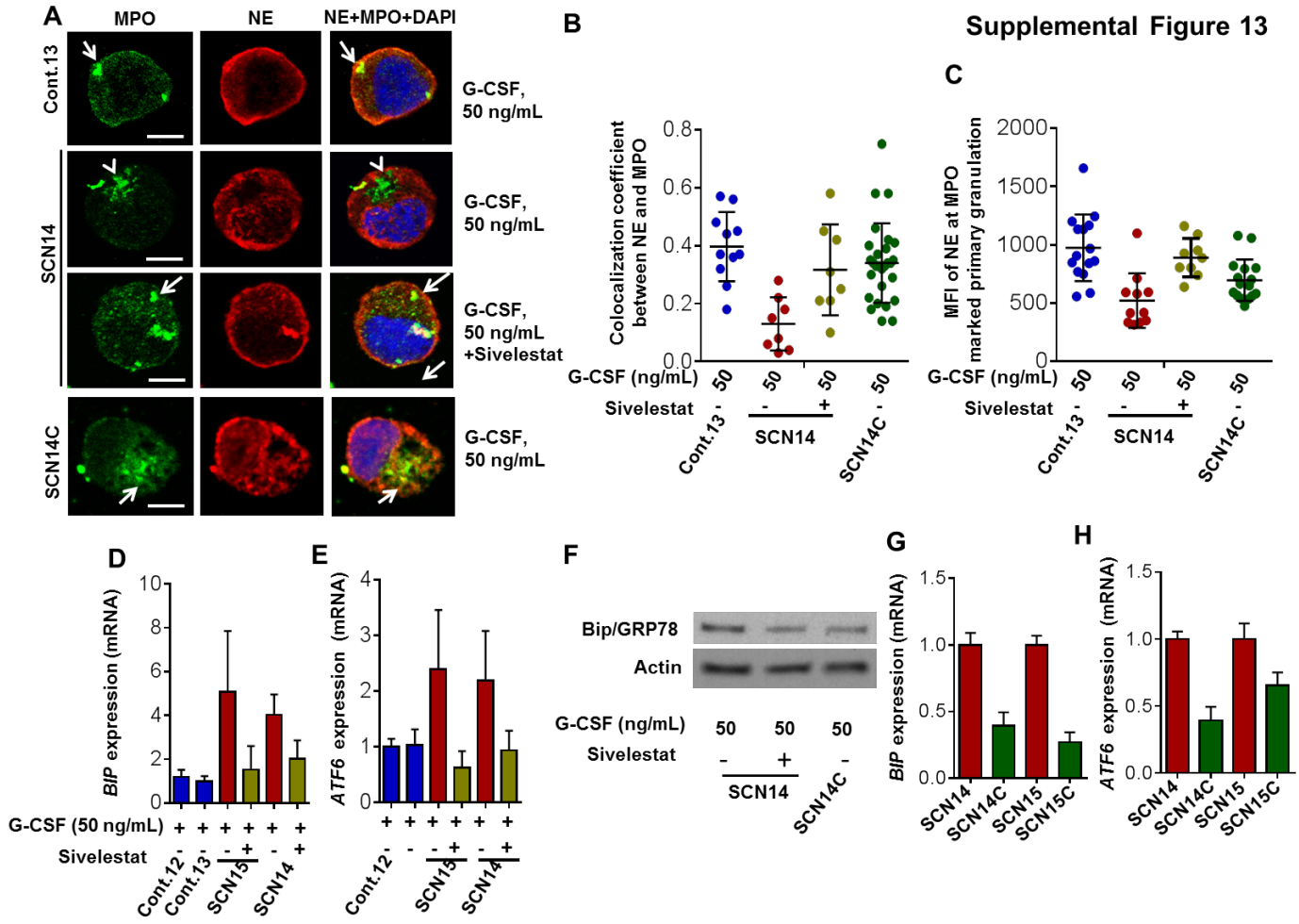

Supplemental Figure 13. Sivelastat rescues the mislocalization of NE and reduces UPR/ER stress in *ELANE* exon 3 mutant derived promyelocytes. (A) Confocal microscopic localization of primary neutrophil granule proteins neutrophil elastase (NE) and myeloperoxidase (MPO) in control (Cont.13), SCN14 and SCN14C iPSC-derived promyelocytes. Arrows indicate the co-localization of NE and MPO in primary granules. Arrowheads indicate the absence of NE in the MPO marked primary granules (bar = 10 μm). Right column show overlay photographs of same fields of NE, MPO and DAPI staining. (B) Quantitation of the correlation of co-localization coefficient between NE and MPO in the primary granules in C. Individual data of 8 or more cells from two independent experiments are presented as mean ± SD. (C) Mean fluorescence intensity of NE at MPO marked primary granules. Individual data of 8 or more cells from two independent experiments are presented as

mean ± SD. (D-E) Quantitative RT-PCR analyses of the expression of UPR pathway genes *BIP* (D) and *ATF6* (E). (F) Western blot of UPR/ER stress marker protein BIP in the promyelocytes/myelocytes derived from SCN14 iPSC cultured in presence or absence of Sivelestat, and from SCN14C iPSC. (G-H) Quantitative RT-PCR analyses of the expression of *BIP*(G) and *ATF6*(H) in the promyelocytes/myelocytes derived from SCN14, SCN15, SCN14C and SCN15C iPSC lines. Data are presented as mean+/-S.D of 2 or more independent experiments in duplicate.

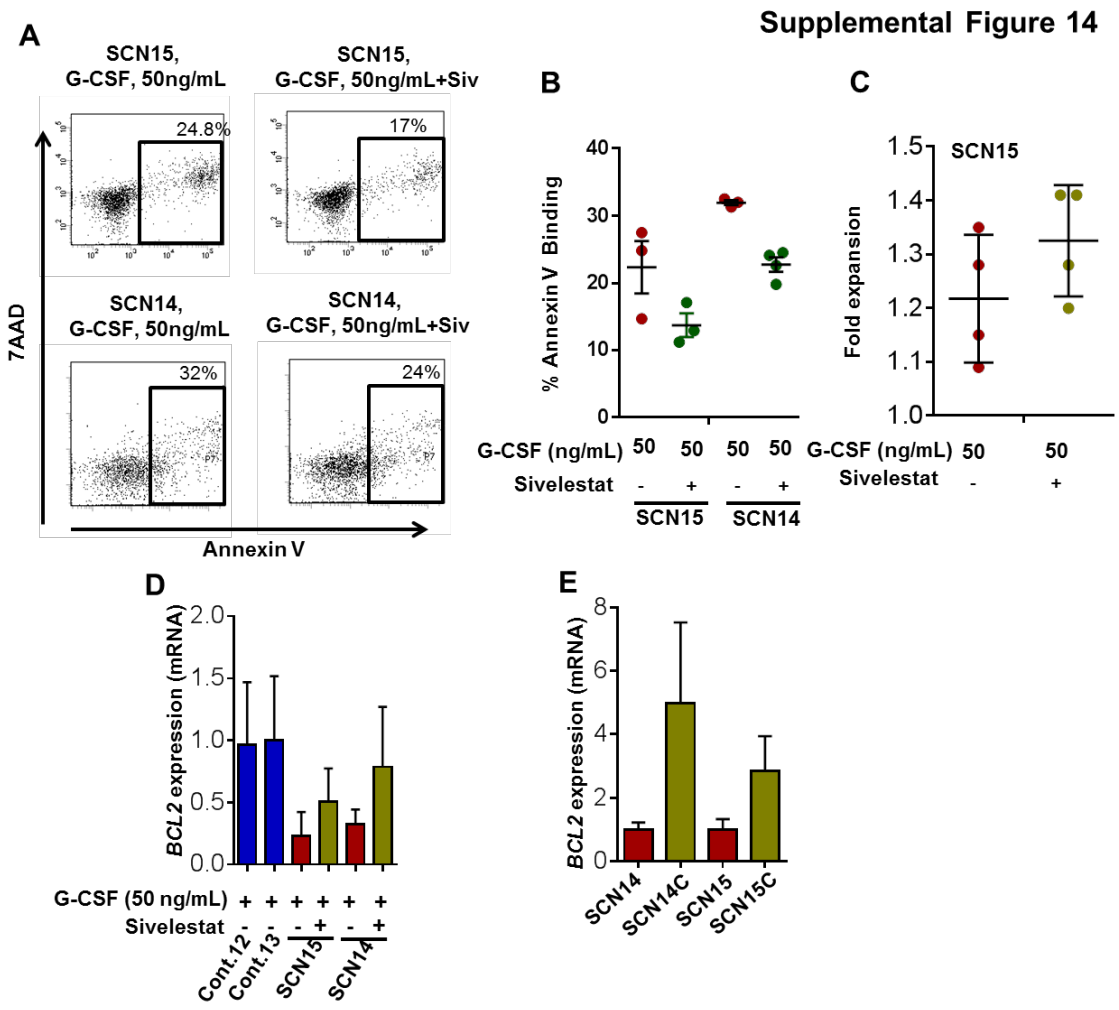

Supplemental Figure 14. Sivelestat increases the survival of SCN 14 and SCN 15 iPSC derived myeloid cells. (A) FACS dot plot showing Annexin-V binding of the myeloid cells derived from SCN15 and SCN14 iPSC lines cultured in presence or absence of Sivelestat. (B) Quantitation of the annexin-V binding of the myeloid cells derived from SCN15 and SCN14 iPSC lines cultured in presence or absence of Sivelestat, and presented as mean ± SD of 3 independent experiments. (C) Fold expansion of $CD45^{+}$ granulocytic precursors in presence 50 ng/mL G-CSF in presence or absence of sivelestat for terminal differentiation assessment. Values of 2 independent experiments performed in duplicate are presented as mean± SD. (D) Quantitative RT-PCR analysis of the expression of *BCL2* in SCN iPSC derived promyelocytes/myelocytes cultured in presence or absence of Sivelestat. (E) Quantitative RT-

PCR analysis of the expression of *BCL2* in the promyelocytes/myelocytes derived from SCN iPSC and mutation corrected iPSC lines. Data are presented as mean-± SD. of 2 or more independent experiments in duplicates.